Applied Physics Express

The Japan Society of Applied Physics

LETTER

Amplified spontaneous emission of phonons as a likely mechanism for density-dependent velocity saturation in GaN transistors

To cite this article: Jacob B. Khurgin *et al* 2016 *Appl. Phys. Express* **9** 094101

View the article online for updates and enhancements.

Related content

- Hot-phonon lifetime in Al0.23 Ga0.77N/GaN channels
  J Liberis, M Ramonas, E Šermukšnis et al.
- Rigid ion model of high field transport in GaN
  Shinya Yamakawa, Richard Akis, Nicolas Faralli et al.
- Hot phonons in high-field transport
  B K Ridley

This content was downloaded from IP address 128.146.189.81 on 13/02/2019 at 20:44

Applied Physics Express **9**, 094101 (2016)
http://doi.org/10.7567/APEX.9.094101

Amplified spontaneous emission of phonons as a likely mechanism for density-dependent velocity saturation in GaN transistors

Jacob B. Khurgin[1], Sanyam Bajaj[2], and Siddharth Rajan[2]

[1]*Department of Electrical and Computer Engineering, Johns Hopkins University, Baltimore, MD 21218, U.S.A.*
[2]*Department of Electrical and Computer Engineering, The Ohio State University, Columbus, OH 43210, U.S.A.*

Received June 14, 2016; accepted July 13, 2016; published online July 29, 2016

We show that density-dependent velocity saturation in a GaN high electron mobility transistor (HEMT) can be related to the stimulated emission of longitudinal optical (LO) phonons. As the drift velocity of electrons increases, the drift of the Fermi distribution in reciprocal space results in population inversion and gain for the LO phonons. Once this gain reaches a threshold value, the avalanche-like increase in LO phonon emission causes a rapid loss of electron energy and momentum and leads to drift velocity saturation. Our simple model correctly predicts both the general trend of decreasing saturation velocity with increasing electron density, and the measured experimental values of saturation.
© 2016 The Japan Society of Applied Physics

High electron mobility transistors (HEMTs) based on GaN and other group III nitrides are among the most promising devices for high power amplification in the RF region, extending all the way to hundreds of GHz.[1–4] GaN is a wide bandgap material with insignificant non-parabolicity and a satellite valley that is removed from the conduction band edge by as much as 1.4 eV. Hence, neither non-parabolicity nor inter-valley transfer can cause velocity saturation (VS). GaN is also a polar material with strong coupling between longitudinal optical (LO) phonons and electrons. It is expected that once the kinetic energy $m_c v_d^2/2$ of the electrons moving with drift velocity v_d approaches the energy $\hbar\omega_{LO} \approx 92$ meV of the optical phonon, LO phonon emission should cause saturation of the velocity near $v_{max} \approx 4 \times 10^7$ cm/s, which is larger than the saturation velocities in narrow bandgap III–V semiconductors.[5] However, experimental data indicate that velocity saturates at lower values, in particular when the carrier concentration is high.[1–4] Recently we carried out a rigorous experimental study of VS in a GaN channel as a function of carrier concentration,[6] and found that saturation velocity v_{sat} steadily decreases from about 1.9×10^7 cm/s to less than 1.0×10^7 cm/s as the sheet density n_s of carriers in the channel increases from 0.8×10^{12} cm^{-2} to about 8.0×10^{12} cm^{-2}. High power operation of a HEMT requires a high carrier density; hence, it is critical to understand the origin of the density dependence of VS and, based on the knowledge gained, develop means of mitigating the factors that cause the saturation velocity to plunge at high carrier densities.

In the course of the last decade, consensus has been that VS in III–nitrides is caused by hot LO phonons, which are generated by electron–phonon scattering and remain in the channel due to their low velocity and relatively long lifetime τ_p.[7–11] The latter can be as long as a few picoseconds[12,13] because the energy of an LO phonon is so high that it cannot efficiently decay into two acoustic phonons,[14] and instead less efficiently decays into a combination of transverse optical (TO) and acoustic phonons.[15] It should be noted that indirect measurement of LO phonon lifetime using anti-Stokes Raman[16] and microwave noise[17,18] measurements indicated the reduction of τ_p with increasing electron density n_s, but that in Ref. 19 we have shown that at high n_s, LO phonons only get scattered away from the center of the Brillouin zone (BZ), while still remaining in the channel for a few picoseconds. While hot phonons are recognized as the source of VS in III–nitrides, the nature of the exact mechanism causing the saturation remains unsettled. In general, since electrons are in thermal equilibrium with phonons, as the occupation numbers of the LO phonons n_{LO} increase, so does the electron temperature T_e and momentum scattering rate $\tau_m^{-1} \sim (2n_{LO} + 1)$, while the energy relaxation rate τ_E^{-1} stays roughly the same, which causes gradual VS. Obviously, n_{LO} increases roughly proportionally to the 3D density of carriers n_e; hence, as shown in Ref. 8, the saturation velocity should decrease as roughly $v_{sat} \sim n_e^{-1/2}$. The measurements performed in Ref. 6 agree qualitatively with the theory developed in Ref. 8, but cannot be approximated by the simple power dependence over the entire range of electron densities. Furthermore, this theory[8] predicts a rather gradual, "soft" velocity vs field dependence, rather than the hard clamping of velocity observed experimentally. One way to determine the saturation velocity would be to perform full Monte-Carlo simulations,[20] which are time consuming, depend on a large number of input parameters, and often do not reveal the clear physical picture behind the observed effects. Thus, a simple model capable of providing a realistic estimate of saturation velocity and its dependence on carrier density would be a welcome addition to the existing means of predicting the performance of III–nitride devices. In this letter we propose such a model, in which VS occurs when the probability of stimulated emission of LO phonons exceeds a certain threshold value determined by the LO phonon lifetime. Using this model and a very limited number of device/material parameters, we succeed in predicting values of $v_{sat}(n_s)$ that are very close to the experimental data obtained in Ref. 6. The "clamping" of the drift velocity above the threshold is strikingly similar to the clamping of population inversion in lasers; hence one may refer to the mechanism responsible for VS as "phonon lasing".[21,22]

In prior work,[7,8] momentum and energy relaxation rates have been estimated under the assumption that the equilibrium distribution of electrons in the conduction band is described by the Fermi–Dirac (FD) function $f_0(\boldsymbol{k}) = \{\exp[(k^2 - \mu)/T_e] + 1\}^{-1}$, shown in Fig. 1(a), where all the variables have been normalized as follows: energies including chemical potential μ to LO phonon energy $\hbar\omega_{LO}$, electron temperature T_e to $T_0 = \hbar\omega_{LO}/k_B = 1060$ K, and the wavevector k to $q_0 = (2m_0\omega_{LO}/\hbar)^{1/2} = 0.68$ nm^{-1}. If one now considers the scattering of LO phonons between the state $\boldsymbol{k}_1$ with energy E_1 and state $\boldsymbol{k}_2$ with energy $E_2 = E_1 - \hbar\omega_{LO}$, the net probability of

 © 2016 The Japan Society of Applied Physics

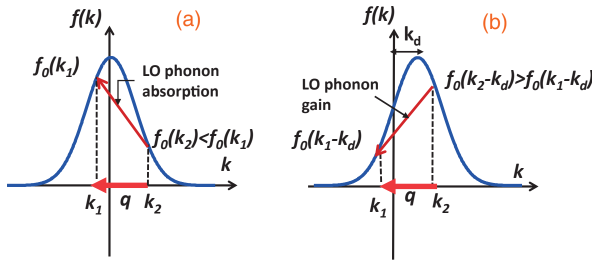

Fig. 1. Electron distribution in the BZ using the standard (a) and drifted (b) FD functions, which results in absorption (a) or gain (b) for LO phonons.

emitting an LO phonon with wavevector $\boldsymbol{q} = \boldsymbol{k}_1 - \boldsymbol{k}_2$ can be written as $R_{12} = 2\pi\hbar^{-1}M^2(R_{\rm sp} + R_{\rm stim})$, where $R_{\rm sp} = f_0(\boldsymbol{k}_1)[1 - f_0(\boldsymbol{k}_2)]$ is the spontaneous emission term, $R_{\rm st} = [f_0(\boldsymbol{k}_1) - f_0(\boldsymbol{k}_2)]n_{\boldsymbol{q}}$ is the stimulated emission term, $n_{\boldsymbol{q}}$ is the occupation number of the LO phonons, $M = q^{-1}(e^2\hbar^2/\varepsilon' 4m_{\rm c}V)^{1/2}$ is the matrix element of electron–phonon interaction, $1/\varepsilon' = 1/\varepsilon_\infty - 1/\varepsilon$, and ε, ε_∞ are values of static and infrared dielectric permittivity respectively. Since state 1 has higher energy than state 2, $f_0(\boldsymbol{k}_1) < f_0(\boldsymbol{k}_2)$ and phonon absorption dominates phonon emission. However, using the equilibrium distribution centered at $\boldsymbol{k} = 0$ to describe the parameters of an electron gas moving with an average drift velocity $\boldsymbol{v}_{\rm d}$ cannot be a good fit with reality, especially when the value of $\boldsymbol{v}_{\rm d}$ becomes comparable to the Fermi velocity. Therefore it is more prudent to use a drifted FD distribution that is shifted in k-space by $\boldsymbol{k}_{\rm d} \equiv \boldsymbol{v}_{\rm d}$, where the drift velocity is normalized to the value $v_{\rm max} = \hbar q_0/m_{\rm c} = 4 \times 10^7$ cm/s defined above. The drifted FD distribution is valid as long as the carrier–carrier scattering time $\tau_{\rm e\text{-}e}$ is as short as the LO phonon scattering time. For carrier concentrations of $5 \times 10^{18}\,{\rm cm}^{-3}$ one can estimate $\tau_{\rm e\text{-}e} < 10$ fs, and hence the drifted FD distribution

$$f(\boldsymbol{k}, \boldsymbol{v}_{\rm d}) = f_0(\boldsymbol{k} - \boldsymbol{v}_{\rm d}) = (\exp\{[(\boldsymbol{k} - \boldsymbol{v}_{\rm d})^2 - \mu]/T_{\rm e}\} - 1)^{-1} \quad (1)$$

as shown in Fig. 1(b) is a valid approximation. For small $v_{\rm d}$ the stimulated emission term remains negative, but for larger values [as shown in Fig. 1(b)] and sufficiently large phonon wavevectors the condition $f(\boldsymbol{k}_1) > f(\boldsymbol{k}_2)$ can be reached. This condition can, of course, be described as population inversion between the two states, and once it is met for a large number of pairs of states $\boldsymbol{k}, \boldsymbol{k} - \boldsymbol{q}$, the total stimulated emission rate for the population of LO phonons

$$R_{\boldsymbol{q},\rm st} = 2\sum_{\boldsymbol{k}} 2\pi\hbar^{-1}M^2_{\boldsymbol{k},\boldsymbol{k}-\boldsymbol{q}}\delta(E_{\boldsymbol{k}} - E_{\boldsymbol{k}-\boldsymbol{q}} - 1)/\hbar\omega_{\rm LO}$$
$$\times [f(\boldsymbol{k}) - f(\boldsymbol{k} - \boldsymbol{q})]n_{\boldsymbol{q}} = G_{\boldsymbol{q}}n_{\boldsymbol{q}} \quad (2)$$

becomes positive, indicating that the phonons experience gain $G_{\boldsymbol{q}} > 0$. The LO phonons whose $\boldsymbol{q}$-vector is parallel to $\boldsymbol{v}_{\rm d}$ will experience the largest population inversion. For these phonons, choosing the polar axis along $v_{\rm d}$ and introducing the shifted wavevector $\boldsymbol{k}' = \boldsymbol{k} - \boldsymbol{v}_{\rm d}$ allows one to re-write the delta function in Eq. (2) as

$$\delta(\cos\theta - (k'_{\rm min} + v_{\rm d})/(k' + v_{\rm d}))/(k' + v_{\rm d})q,$$

where θ is the polar angle of $\boldsymbol{k}'$ and $k'_{\rm min} = 1/2(q + q^{-1}) - v_{\rm d}$. Going from summation to integration we then obtain for the temporal gain $G_q = G_0 q^{-3}\int_{k_{\rm min}}^{\infty}(f_k - f_{k-q})(k^2/k + v_{\rm d})\,dk$, where we introduce $G_0 = e^2 q_0/4\pi\varepsilon'\hbar = \alpha_0(\varepsilon_0/\varepsilon')q_0 c = = 1.2 \times 10^{14}\,{\rm s}^{-1}$ and have dropped the prime symbol in the integral. In the new notation, $f_k = \{\exp[(k^2 - \mu)/T_{\rm e}] + 1\}^{-1}$

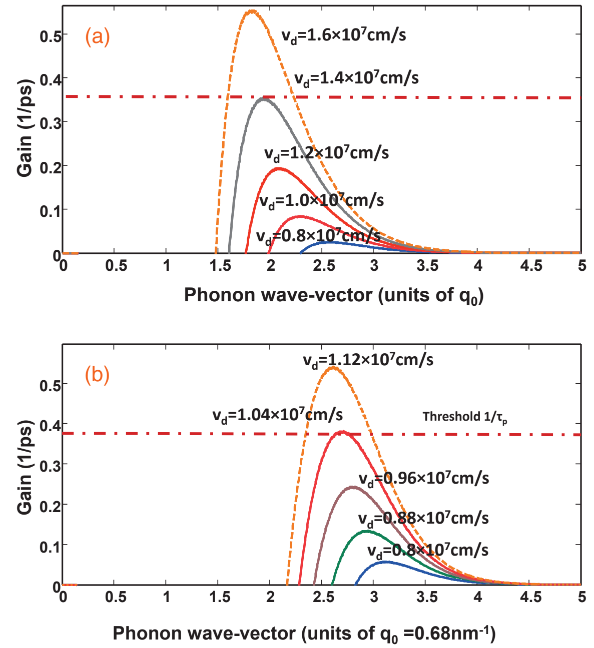

Fig. 2. Wave vector dependence of the LO phonon gain G_q for two different electron densities, (a) $N_{\rm e} = 5 \times 10^{18}\,{\rm cm}^{-3}$ and (b) $N_{\rm e} = 5 \times 10^{18}\,{\rm cm}^{-3}$.

and $f_{k-q} = (\exp\{[k^2 + q^2 - 2kq(k_{\rm min} + v_{\rm d})/(k + v_{\rm d}) - \mu]/T_{\rm e}\} + 1)^{-1}$; hence the population inversion condition $f_k > f_{k-q}$ is $1/2(q + q^{-1}) - v_{\rm d} < k < q^2 v_{\rm d}$, indicating that it can occur only when $q > 1/2v_{\rm d}$. Thus, it is expected that for small $v_{\rm d}$, only large momentum LO phonons can experience gain, and this gain is small; however, as $v_{\rm d}$ increases, the gain spectrum spreads towards smaller q values and the gain value increases. The gain obviously increases with $n_{\rm e}$, as the relation between the chemical potential μ and $n_{\rm e}$ (normalized to the density of electrons with a Fermi wavevector equal to q_0, $n_0 = 1/3\pi^2 q_0^3 = 1.1 \times 10^{19}\,{\rm cm}^{-3}$) is

$$n_{\rm e} = 3\int\{\exp[(k^2 - \mu)/T_{\rm e}] + 1\}^{-1}k^2\,dk.$$

The results from calculating G_q for two different three-dimensional (3D) densities of electrons $N_{\rm e} = 5 \times 10^{18}\,{\rm cm}^{-3}$ ($n_{\rm e} = 0.45$) and $N_{\rm e} = 3 \times 10^{19}\,{\rm cm}^{-3}$ ($n_{\rm e} = 2.7$) are shown in Figs. 2(a) and 2(b) respectively. In both cases the gain, which is confined to the relatively narrow region of phonon wavevectors, becomes noticeable at velocities approaching 2×10^6 cm/s ($v_{\rm d} \sim 0.2$ relative to $v_{\rm max}$). As $v_{\rm d}$ increases, both the width and peak value of the gain increase rapidly, as the peak slowly shifts towards smaller q values. The gain increases faster with higher $n_{\rm e}$, as can be seen in Fig. 3, where peak phonon gain is plotted as a function of $v_{\rm d}$ for four different $n_{\rm e}$ for an assumed $T_{\rm e}$ of 1030 K. Electrically driven phonon gain was previously predicted in GaAs-based QW's,[23–25] but in GaN, electron–phonon coupling M^2 is almost an order of magnitude higher and the phonon lifetime is longer, hence the chances of observing stimulated LO emission are greatly enhanced.

The rate equation for the phonons can be written as

$$\frac{dn_q}{dt} = G_q n_q + S_q - \frac{n_q - \bar{n}_q}{\tau_{\rm p}} \quad (3)$$

where $\bar{n}_q$ is the equilibrium phonon occupational number at a given lattice temperature, and the rate of spontaneous emission is

© 2016 The Japan Society of Applied Physics

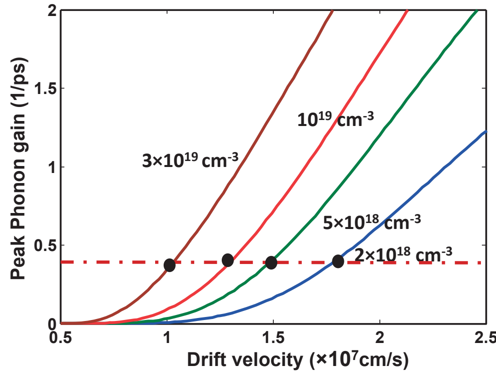

Fig. 3. Peak value of LO phonon gain G_q as a function of drift velocity v_d for different electron densities.

$$S_q = G_0 q^{-3} \int_{k_{min}}^{\infty} f_k(1 - f_{k-q})(k^2/k + v_d)\, dk.$$

Clearly, when the peak gain in Eq. (3) approaches its threshold value τ_p^{-1}, the number of LO phonons starts increasing exponentially. Therefore, as the bias increases all of the additional power transferred from the field to the electrons will then be very efficiently transferred to the LO phonons via a stimulated emission process, and the drift velocity will be clamped at the threshold value exactly as the population inversion in the laser is clamped at the threshold;[26] hence as the term "phonon lasing".[21,22] The major difference from an optical laser in this case is of course the absence of a resonant cavity providing feedback and selecting a single resonant mode. Feedback is absolutely not necessary, however, since LO phonons have small group velocities (even when coupled with plasmons). Furthermore, many lasers are known to operate without a resonator.[27] The mode selection is achieved by the sharp spectrum of the gain itself, and the spatial spectrum of the emitted phonons narrows, once again resembling the behavior of photons in the laser. Whether it is more correct to call the process "lasing" or "amplified spontaneous emission" is an interesting question from the fundamental physics point of view, but it is not directly relevant to this work in which, far from playing a constructive role, the "phonon lasing" acts as a "spoiler" that limits drift velocity and hence negatively affects both the speed and transconductance of HEMTs. If one is to avoid any reference to "lasing", perhaps the term "phonon avalanche" would be the most appropriate.

If we now plot the line corresponding to the threshold gain in Figs. 2 and 3, we can find the values of v_{sat} for different N_e's. The value of the peak gain curve in Fig. 3 increases with carrier density. Therefore, the saturation velocity exhibits a strong dependence on electron density (as well as on phonon lifetime), but at very high densities (in excess of $2 \times 10^{19}\,\text{cm}^{-3}$) the drift velocity is expected to saturate at around $10^7\,\text{cm/s}$ under a wide range of conditions. This can be best seen in Fig. 4(a), where the density dependence of v_{sat} is compared with the experimental values obtained in Ref. 6. Since our model is 3D, the values of N_e were obtained from the measured sheet density N_s via a self-consistent solution of the Poisson and Schrödinger equations. Thus, our simple model achieves good agreement with the experiment, using only a single adjustable parameter ($T_e \sim 1000\,\text{K}$). We have also performed modeling using a two-dimensional electron

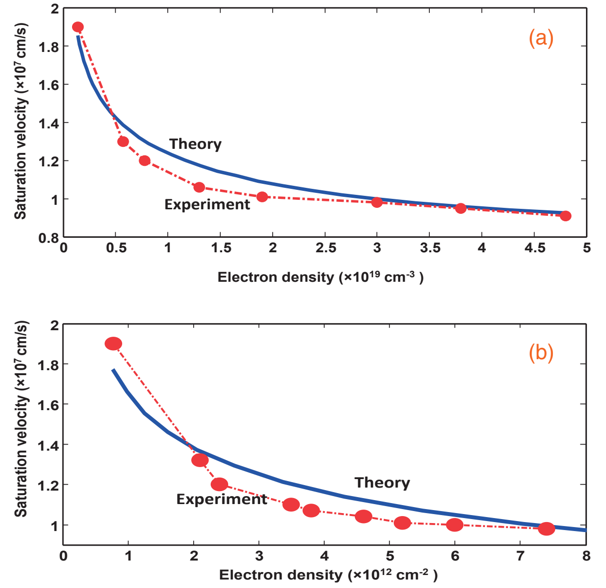

Fig. 4. Saturation velocity in a GaN HEMT as a function of electron density. (a) 3D model. (b) 2D model. Red dots represent experimental data from Ref. 6.

gas (2DEG) in the channel. Since the phonons are 3D, we required the effective channel thickness d_{eff} to determine the volume in which the phonons interacting with the electrons are contained; this was also done via self-consistent solutions to the Poisson and Schrödinger equations. The derivation of the expression for the gain is similar to the one outlined above for the 3D case, and results in

$$G_q = 2G_0 \frac{1}{q^3 d_{eff}} \int_{k_{min}}^{\infty} (f_k - f_{k-q}) \times \frac{k}{\sqrt{(k + v_d)^2 - (k_{min} + v_d)^2}}\, dk, \quad (4)$$

where d_{eff} is scaled by q_0. The results of the calculation are shown in Fig. 4(b) and reproduce the experimental data reasonably well, though not as well as with 3D modeling. This may be due to the fact that the 2D calculations do not take into account the exact shape of the electron wavefunction.

Having shown that the newly introduced "phonon lasing" model predicts the concentration dependence of v_{sat} with a good accuracy, we now explore the dynamics of phonons and carriers at different electric fields without resorting to the complexity of full Monte-Carlo simulations. This can be accomplished by solving the balance equations

$$\frac{dE_k}{dt} = -Fv_d - (3/8\pi n_r) \int [n_{\boldsymbol{q}}(T_e) - \bar{n}_q] d^3\boldsymbol{q} = 0$$

$$\frac{dv_d}{dt} = -F/2 - (3/8\pi n_r) \int [n_{\boldsymbol{q}}(T_e) - \bar{n}_q] q_x d^3\boldsymbol{q} - \mu_{LF}^{-1} v_d = 0 \quad (5)$$

where the kinetic energy E_k is normalized to $\hbar\omega_{LO}$, time to τ_p, the electric field F to $F_0 = \hbar q_0/2e\tau_p = 1.2 \times 10^5\,\text{V/m}$, and the low field mobility (which includes all the scattering mechanisms other than LO phonons) μ_{LF} to $\mu_0 = e\tau_p/m_c = 2.3 \times 10^5\,\text{cm}^2\,\text{V}^{-1}\,\text{s}^{-1}$. With the temperature-dependent n_q obtained from Eq. (3), for each value of v_d, a pair of F and T_e satisfying Eq. (5) can be obtained, resulting in the VS curves shown in Fig. 5(a) for the same carrier densities as in

© 2016 The Japan Society of Applied Physics

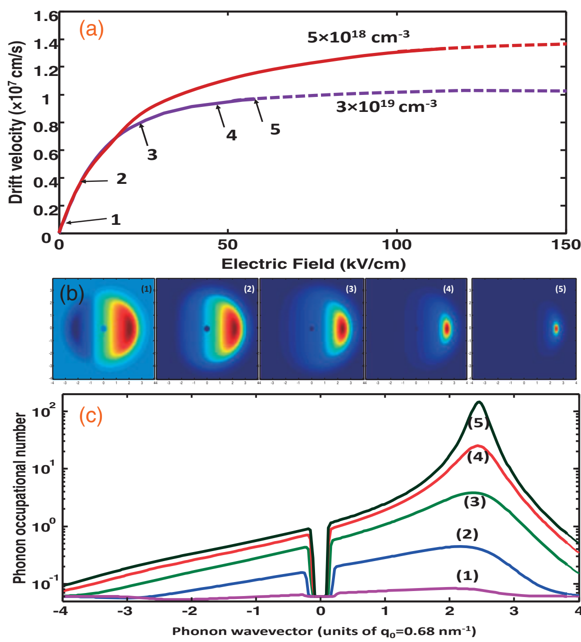

Fig. 5. (a) Velocity vs field curves for a GaN HEMT for two electron densities modeled up to the onset of phonon "lasing" or "avalanche". (b, c) Hot LO phonon distribution in the BZ zone for five regimes indicated in (a).

Fig. 2. The lattice temperature of 350 K and the low-field mobility of 1000 $cm^2 V^{-1} s^{-1}$ is assumed, and the results conform both to the estimates of v_{sat} made above [Fig. 4(a)] and with the experiments in Ref. 6. To illustrate the role played by the stimulated emission of LO phonons, five "snapshots" of LO phonon distribution in the BZ at different drift velocities [as indicated in Fig. 5(a)] are displayed in Fig. 5(b). The values of n_q vs q_x are plotted in Fig. 5(c). As one can see, for small values of v_d the phonon distribution is spread out, but as v_d increases, a narrow peak appears on the q_x axis in which the n_q grows exponentially and v_d saturates.

Our simple model does not predict exactly what happens beyond the saturation point. This is no different from the fact that the behavior of a silicon FET beyond pinch-off requires a more involved description than a textbook FET model.[28] Still, our model faithfully predicts the behavior of GaN HEMTs up to the point where the stimulated emission of LO phonons inside a narrow volume region in reciprocal space becomes the dominant relaxation process. At this point, the carrier scattering rate $\tau_{ee}^{-1} \sim 10^{14} s^{-1}$ is no longer fast enough to replenish the population of forward propagating electrons; hence the carrier distribution is no longer in equilibrium. This is strikingly similar to the "spectral hole burning"[29] phenomenon which occurs in lasers. As a result, the distribution of LO phonons [Fig. 5(b)] is expected to broaden, and the drift velocity is expected to continue to increase slowly, as indicated by the dashed lines in Fig. 5(a).[6] Note that the moderately small discrepancy between our results and the measurements in Ref. 6 can be attributed to the fact that a uniform field distribution along the channel has been assumed. While this assumption is realistic in the absence of the equipotential surface from the gate, further detailed investigation is required to make sure that this assumption is correct.

We consider the feasibility of an experimental confirmation of "phonon lasing" that is more direct than reproduction of the VS curve. The best means for revealing LO phonon existence in the small BZ region is via second order anti-Stokes Raman measurements of the operating HEMT. These experiments are far from trivial, but are within the realm of possibility.[30] We see no practical applications of these hot phonons as of yet, unless the decay of stationary LO phonons can generate directional acoustic THz phonons; this should be investigated in the future. The main practical consequence of this work is the identification of the "lasing-like" stimulated emission of LO phonons as a major factor causing VS in GaN HEMTs. Controlling, or better, preventing the "phonon lasing" by introducing additional LO phonon scattering mechanisms, such as disorder,[31] may lead to improvements in the performance of III–nitride HEMTs.

Acknowledgment The authors gratefully acknowledge the support from DATE MURI (ONR N00014-11-1-0721, Dr. Paul Maki).

1) Y. Yue, Z. Hu, J. Guo, B. Sensale-Rodriguez, G. Li, R. Wang, F. Faria, T. Fang, B. Song, X. Gao, S. Guo, T. Kosel, G. Snider, P. Fay, D. Jena, and H. Xing, IEEE Electron Device Lett. **33**, 988 (2012).
2) K. Shinohara, D. Regan, A. Corrion, D. Brown, Y. Tang, J. Wong, G. Candia, A. Schmitz, H. Fung, S. Kim, and M. Micovic, IEDM Tech. Dig., 2012, 27.2.1.
3) Y. Tang, K. Shinohara, D. Regan, A. Corrion, D. Brown, J. Wong, A. Schmitz, H. Fung, S. Kim, and M. Micovic, IEEE Electron Device Lett. **36**, 549 (2015).
4) S. Dasgupta, D. F. Brown, F. Wu, S. Keller, J. S. Speck, and U. K. Mishra, Appl. Phys. Lett. **96**, 143504 (2010).
5) D. K. Ferry, *Semiconductor Transport* (Taylor & Francis, London, 2001).
6) S. Bajaj, O. F. Shoron, P. S. Park, S. Krishnamoorthy, F. Akyol, T.-H. Hung, Sh. Reza, E. Chumbes, J. Khurgin, and S. Rajan, Appl. Phys. Lett. **107**, 153504 (2015).
7) B. K. Ridley, W. J. Schaff, and L. F. Eastman, J. Appl. Phys. **96**, 1499 (2004).
8) J. Khurgin, Y. Ding, and D. Jena, Appl. Phys. Lett. **91**, 252104 (2007).
9) J. H. Leach, C. Y. Zhu, M. Wu, X. Ni, X. Li, J. Xie, Ü. Özgür, H. Morkoç, J. Liberis, E. Šermukšnis, A. Matulionis, H. Cheng, and Ç. Kurdak, Appl. Phys. Lett. **95**, 223504 (2009).
10) G. P. Srivastava, Phys. Rev. B **77**, 155205 (2008).
11) G. P. Srivastava, J. Phys.: Condens. Matter **21**, 174205 (2009).
12) K. T. Tsen, D. K. Ferry, A. Botchkarev, A. Serdlov, A. Salvador, and H. Morkoc, Appl. Phys. Lett. **72**, 2132 (1998).
13) L. Shi, F. A. Ponce, and J. Menendez, Appl. Phys. Lett. **84**, 3471 (2004).
14) P. G. Klemens, Phys. Rev. **148**, 845 (1966).
15) B. K. Ridley, J. Phys.: Condens. Matter **8**, L511 (1996).
16) K. T. Tsen, J. G. Kiang, D. K. Ferry, and H. Morkoc, Appl. Phys. Lett. **89**, 112111 (2006).
17) A. Matulionis, J. Liberis, I. Matulionienė, M. Ramonas, L. F. Eastman, J. R. Shealy, V. Tilak, and A. Vertiatchikh, Phys. Rev. B **68**, 035338 (2003).
18) A. Matulionis, J. Liberis, E. Šermukšnis, J. Xie, J. H. Leach, M. Wu, and H. Morkoç, Semicond. Sci. Technol. **23**, 075048 (2008).
19) J. B. Khurgin, S. Bajaj, and S. Rajan, Appl. Phys. Lett. **107**, 262101 (2015).
20) M. Ramonas and A. Matulionis, Semicond. Sci. Technol. **19**, S424 (2004).
21) R. P. Beardsley, A. V. Akimov, M. Henini, and A. J. Kent, Phys. Rev. Lett. **104**, 085501 (2010).
22) I. S. Grudinin, H. Lee, O. Painter, and K. J. Vahala, Phys. Rev. Lett. **104**, 083901 (2010).
23) S. M. Komirenko, K. W. Kim, V. A. Kochelap, I. Fedorov, and M. A. Stroscio, Appl. Phys. Lett. **77**, 4178 (2000).
24) S. M. Komirenko, K. W. Kim, V. A. Kochelap, I. Fedorov, and M. A. Stroscio, Phys. Rev. B **63**, 165308 (2001).
25) W. Liang, K. T. Tsen, O. F. Sankey, S. M. Kornienko, K. W. Kim, V. A. Kochelap, M.-C. Wu, and H. Morkoc, Appl. Phys. Lett. **82**, 1968 (2003).
26) A. E. Siegman, *Lasers* (University Science Books, Sausalito, CA, 1996).
27) G. Smith, P. Shardlow, and M. Damzen, Opt. Lett. **32**, 1911 (2007).
28) D. A. Neamen, *Semiconductor Physics and Devices* (McGraw-Hill, New York, 2012).
29) O. Svelto and D. C. Hanna, *Principles of Lasers* (Plenum, New York, 2010).
30) G. Xu, S. K. Tripathy, Y. J. Ding, Y. Cao, K. Wang, D. Jena, and J. B. Khurgin, Laser Phys. **19**, 745 (2009).
31) J. B. Khurgin, D. Jena, and Y. J. Ding, Appl. Phys. Lett. **93**, 032110 (2008).

 © 2016 The Japan Society of Applied Physics